*ASGE Vol. 06 (01), pp. 1-13, 2022*

Egyptian Knowledge Bank

***International Journal of Advances in Structural and Geotechnical Engineering***

*https://asge.journals.ekb.eg/*

*Print ISSN 2785-9509* *Online ISSN 2812-5142*

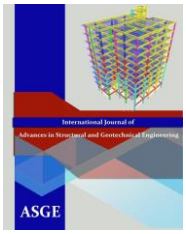


# AN ANCHORAGE TECHNIQUE FOR FLEXURAL STRENGTHENING OF RC BEAMS USING NSM BFRP BARS

**Hesham M. Diab**

*Associate Professor, Faculty of Engineering, Assiut University, Assiut, Egypt*
*E-mail:* diab@aun.edu.eg

## ABSTRACT

Near-surface mounted (NSM) fiber reinforced polymer (FRP) bars are becoming increasingly effective in strengthening and upgrading reinforced concrete (RC) beams. Most of the previous related works indicated that failure of the NSM FRP-strengthened beam was due to premature debonding failure. In this study, embedded through-section (ETS) end anchorage technique is introduced to increase the flexural capacity of RC beams strengthened with NSM basalt fiber-reinforced polymer (BFRP) bars. The ETS end anchorage technique was manually developed by forming a bent part with angle 45o at the ends of basalt FRP bars using BFRP bars and sheet. Five RC rectangular beams were prepared and tested. One specimen was kept as an unstrengthened beam as a reference. Two specimens were strengthened with NSM BFRP bars using ETS end anchorage, whereas the remaining two specimens were strengthened utilizing NSM BFRP bars without anchorages. The axial stiffness of BFRP bars was kept constant for all strengthened beams. The beams were subjected to a four-point bending test until failure, and the results were evaluated. The experimental results revealed that using the proposed non-mechanical anchor significantly enhance the flexural capacity and post-yield stiffness of NSM BFRP-strengthened beams. Moreover, ETS end anchorage achieved 90% of the ultimate tensile capacity of the BFRP bars. The surface area of BFRP reinforcement and the number of the end anchorages had a significant impact on the load capacity of the strengthened beams

**Keywords:** Near-surface mounted (NSM), Basalt FRP bars, RC beams, Flexural strengthening, Embedded through-section (ETS) end anchorage, Nonmechanical anchor.

## INTRODUCTION

Using near-surface mounted (NSM) fiber reinforced polymer (FRP) bars is an appealing technique to enhance flexural capacity of flexural deficient RC members. Compared to conventional external bonding (EB) FRP methods, this near-surface mounted (NSM) FRP strengthening system (1) provided stronger FRP-concrete bonds, (2) ensured a better protection for FRP reinforcements against fire or vandalism, and (3) demanded less preparation works after grooving [1,2]. Although debonding failure is less expected to occur in NSM FRP reinforcement compared to EB FRP sheets [3,4], previous studies have reported that NSM FRP methods have not been able to guarantee that the tensile strength of FRP reinforcements is fully developed, because of premature debonding of epoxy and concrete splitting [5,6]. Thus, substantial research has been conducted to investigate the bond performance of NSM FRP reinforcements in concrete [7,8]. Despite useful recommendations enhancing the bond capacity of NSM FRP reinforcements, debonding failure problems remain the key issue to enhanced RC structures using the NSM-FRP technique.[٣]

The favorable flexural failure mode of strengthened beams is attributable to either concrete crushing or tensile rupture of FRP reinforcement, and necessary precautions should be taken to delay or avoid the other two failure modes: shear failure and FRP debonding [9]. Researches were dedicated to finding suitable anchorage systems to delay or prevent the premature debonding failure of the NSM FRP technique. Although many studies were committed to providing a suitable anchorage system for structures strengthened with FRP sheets/plates [10-13], NSM-FRP anchorage systems are a relatively new research field [13-18]. Different anchorage systems for NSM FRP flexural strengthening were used as follows: metallic anchorages; U-shaped FRP/steel hoops; fully wrapped through beams; patch anchors using bidirectional fibers; mechanical substrate strengthening. The effect of U-shaped FRP/steel Hoopes as end anchors of NSM FRP strips/bars was investigated by Wu et al. [19] and Peng et al. [20]. These anchors managed to effectively prevent premature end debonding and increase the ductility of the beams, but a slight increase in the ultimate flexural capacity was observed. Recently, Wang et al. [13, 18] introduced an innovative additional ribs anchorage system for NSM FRP bars to suspend the debonding failure. Using direct pullout specimens, they noticed that the developed anchorage system improved the bond capacity and enhanced the anchorage performance of the NSM FRP bars.

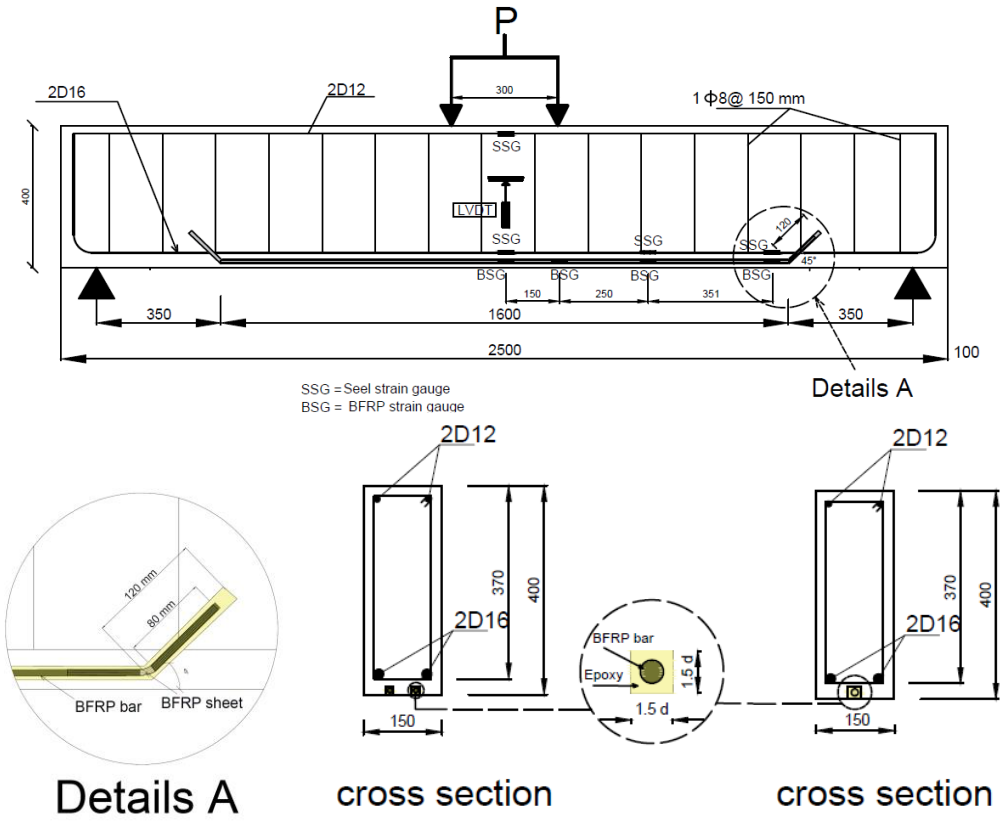


**Fig. 1: Tested beam details**

Embedded through-section (ETS) technique is a developed strengthening method to improve the shear capacity of RC beams using FRP bars [21-22]. The ETS method involves bonding the FRP bars to the concrete core through holes created along the beam web. It was mentioned that this technique improves the reinforcement-concrete bonding by ensuring that the embedded FRP bars are highly confined by concrete.

Diab and Sayed [23] developed an embedded through-section (ETS) end anchorage technique to increase the shear capacity of RC T-beams using NSM BFRP bars. The end of the BFRP bar is installed in a vertical hole made in the slab next to the web of the beam filled with epoxy to create the ETS end anchorage. This anchorage technique has several advantages compared to conventional anchorage methods in terms of being less time-consuming and having fewer requirements for surface preparation or skilled works. Moreover, the ETS end anchorage relies

on the concrete core of the RC beam, which offers greater confinement, hence improving bonding performance .

Despite the attractive merits of the ETS end anchorage method in shear strengthening, it cannot be used in the flexural strengthening of RC beams. The commercial FRP rebars are generally made by thermoset materials which cannot be bent into hooks like steel rebars [24]. Therefore, usage of these unbendable FRP bars as NSM flexural reinforcement methods narrowed anchorage possibility down to manually manufacturing FRP rebars [15,25]. Reda et al. [15] used GFRP bars with bent ends fabricated at the laboratory from roving glass fiber strands bonded together with a resin to increase the bond capacity of the NSM bars.

This study aims to propose an FRP manually made end anchorage using the ETS technique for RC beams strengthened in flexure with commercial BFRP bars using the NSM technique. This study investigates the effect of the following variables: (1) the presence of ETS end anchorage; (2) BFRP rebars in flexural strengthening; (3) the effect of the surface area of BFRP with the same axial stiffness of BFRP rebars.

(a) After removing the wooden stick from specimens and cleaning the grooves

(b) grooves filled with 2/3 epoxy adhesive and installing BFRP bars

(c) filling grooves with epoxy adhesive

**Fig. 2: Application of NSM BFRP strengthening method for RC beams**

# EXPERIMENTAL PROGRAM

### Description of the specimens

The experimental program consists of five RC beams. Tested beams have the same dimensions and internal reinforcement arrangements. The cross-section geometry and details of steel reinforcement of the tested beams are shown in Fig. 1. All beams are 2500 mm long (2300 mm, the effective span), 150 mm in width, and 400 mm in depth (370 mm, the effective depth). The bottom longitudinal steel reinforcement consists of two ribbed bars, 16 mm in diameter, which were anchored at support with 90o hooks at both sides to achieve the anchorage criteria. The top reinforcement included two ribbed bars, 12 mm in diameter. The steel stirrups are 8 mm in diameter distributed along the beam with a space of 150 mm .

**Table 1: Mechanical properties of reinforcement**

| Diameter (mm) | Type | $f_y$ (MPa) | $f_u$ (MPa) | E (GPa) | Usage |
|---|---|---|---|---|---|
| Ø 8 | Mild | ٣٠٨ | ٤٠٠ | 200 | Stirrups |
| Φ 12 | High tensile | 429 | 620 | 200 | Comp. steel |
| Φ 16 | High tensile | ٤٣٧ | 638 | 203 | Tension steel |

**Materials properties**

The beams were cast using concrete with a target compressive strength of 25 MPa. The 28-day compressive strength (Fcu) was obtained using standard cubes (150x150x150 mm). The average compressive strength was 27.5 MPa. The properties of longitudinal and transverse steel reinforcement are shown in Table 1. These properties were obtained according to ASTM A370-97a [26] and Egyptian code [27]. Two types of basalt fiber reinforced polymer (BFRP) composites were used in this study. The first one was GBF® BFRP bars (BFRP-10 and BFRP-14) manufactured by China GBF [28]. The other type was the BUF7-300 basalt sheet manufactured by Shanxi Basalt Fiber Technology Co. [29] which was adopted for making the embedded through-section (ETS) end anchor.

Characteristics of the BFRP bars and BFRP sheet are shown in Table 2, provided by manufacturers. A two-part epoxy (Sikadur® 30) was used as the adhesive filler to fix the BFRP bars inside the grooves and a two-part adhesive (Sikadur® 330) employed to wrap the BFRP sheet around the BFRP bars to form the ETS anchor. Table 3 presents the properties of the epoxies provided by the manufacturer.[٣٠,٣١]

**Table 2: Mechanical properties of the BFRP materials**

| Basalt Types | Weight (g/m/) for bars or (g/m2) for sheet | Diameter or thickness (mm) | Tensile strength (MPa) | Tensile modulus (GPa) | Rupture strain (%) |
|---|---|---|---|---|---|
| BFRP-10 | 162 | 10 | 1200 | 52 | 2.31 |
| BFRP-14 | 307 | 14 | 1000 | 48 | 2.08 |
| Basalt (BUF7-300) | 300 | 0.170 | 2100 | 91.0 | 2.60 |

**Strengthening system**

Four RC beams were strengthened using NSM BFRP Technique. The NSM BFRP strengthening technique is illustrated in Fig. 2(a to c). The following steps have been taken to apply this system: (1) grooves with square section (width 1.5 times the diameter of the BFRP bar) were made in the concrete cover of the RC beams using one or two rectangular wooden sticks attached to the wooden frameworks to locate grooves for NSM BFRP bars; (2) after removing the wooden sticks from concrete specimens, the surface of grooves was grinded to increase the friction between adhesive and concrete; (3) the grooves were cleaned with compressed air and acetone and filled with 2/3 the epoxy adhesive (Sikadur® 30) required; (4) the BFRP bars were installed in the grooves; (5) the grooves were filled with epoxy adhesive and the surface was leveled. If the ETS end anchorage was to be installed, the following steps shown in Fig. 3(a and b) were taken: (1) inclined holes (with 1.5 times the diameter of the BFRP bar) were drilled by a masonry drill into the cross-section of the beam to 120 mm depth at the required locations; (2) the holes were cleaned by compressed air and filled with 2/3 of the needed epoxy adhesive volume required; (3) the handmade bent ends (with 45o angle) of the BFRP bar were inserted into the inclined holes to create the ETS end anchorage .

To overcome the bending problem of the commercial BFRP bars, the following procedures shown in Fig. 3(c to f) were adopted to create the inclined ends to the BFRP bars. These ends were created from BFRP sheets with 200x100 mm in dimensions wrapped around BFRP end and part of BFRP rebar with 80 mm to be inserted in the inclined holes. The fiber direction of the BFRP sheet was in the direction of the BFRP bar. Dimensions of each part are presented in Fig. 3c. BFRP sheet was impregnated with epoxy resin and wrapped around both the bar end and the other part of BFRP bar. Theses handmade ends of the BFRP bar were bent to the required angle (45o) as shown in Fig. 3f. Finally, these bent ends were inserted into the predrilled holes through the cross-section of the beam, creating the ETS end anchorage technique as shown in Fig. 4.

**Table 3: properties of the epoxy**

| Epoxy type | Mechanical properties | values |
|---|---|---|
| Epoxy (sikadur® 30 | Ultimate strength (MPa) | 24-27 (15oC); 26-31(35oC) |
| | Shear strength (MPa) | 14-17 (15oC); 16-19(35oC) |
| | Elastic modulus (GPa) | 11.2(23oC) |
| Epoxy (sikadur® 330 | Ultimate strength (MPa) | 30 (23°C) |
| | Tensile adhesion strength (MPa) | Concrete fracture (> 4 N/mm2) on sandblasted substrate |
| | Elastic modulus (GPa) | 4.5(23oC) |

**Test parameters and instrumentation**

This study aims to introduce ETS end anchorage as a suitable technique for general RC beams strengthened in flexure with NSM BFRP bars. In order to achieve this purpose, nominally identical RC beams strengthened with NSM BFRP bars were tested. The axial stiffness of BFRP reinforcement was kept constant for the different strengthened beams; therefore, two types of BFRP bars were used in this study, BFRP-10 and BFRP-14. Two RC beams were strengthened with one BFRP-14 rebar for each one and ETS end anchorage method was applied to one of them. The other two beams were strengthened with two BFRP-10 rebars for each one and the ETS end anchorage method was applied to one of the beams to each rebar. Details and symbols of specimens are listed in Table 4 .

**Table 4: Concrete specimens' details**

| Designation of specimen | Number of NSM BFRP bars | Diam. of Bars (mm) | Anchorage Type | BFRP cross sectional area (mm2) | Axial stiffness ratio $\left(\frac{(A.E)_{BFRP}}{(A.E)_{Steel}}\right)$ |
|---|---|---|---|---|---|
| BC | None | ----- | --- | | --- |
| B1F14_N | 1 Bar | 14 | No | 153 | 0.090 |
| B2F10_N | 2 Bars | 10 | No | 157 | 0.092 |
| B1F14_A | 1 Bar | 14 | ETS end anchorage | 153 | 0.090 |
| B2F10_A | 2 Bars | 10 | ETS end anchorage | 157 | 0.092 |

All the different beams were internally instrumented with four strain gauges attached to the longitudinal steel reinforcement (Fig. 1). Externally, each beam was monitored using one linear variable displacement transducer (LVDT), placed at the midspan of the beams to measure the maximum deflection. Moreover, four strain gauges were attached to BFRP bars at different locations for the strengthened beams (Fig. 1). Four-point bending tests (Fig. 5) were carried out using a 5000 kN capacity hydraulic test machine and the applied load was recorded with a 2000 kN load cell. All the tests were conducted under displacement control conditions at 2 mm/min until failure. The load and instrument signals were computerized and recorded using an automatic data acquisition system at a sampling rate of 1 Hz.

## EXPERIMENTAL RESULTS AND DISCUSSIONS

Table 5 summarizes the test results by listing the following: the ultimate loads of the tested beams (PU); deflection at ultimate load; percentage of ultimate load gain with respect to the control beam (BC); failure mode of the tested beams. The use of NSM BFRP bars improved the flexural capacity of RC beams. The increase in flexural capacity of strengthened beams is

ranging from 17.48% to 42.48% based on the surface area of the BFRP bars and the presence of the ETS end anchorage. The flexural capacity of NSM-BFRP strengthened beams without end anchorage increased by percentages ranging from 17.48% to 31.39% compared to the control Beam. On the other hand, the flexural capacity of NSM-BFRP strengthened beams with end anchorage increased by percentages ranging from 23.95% to 42.48% compared to the control Beam. The increase in flexural capacity of the BFRP-strengthened beams emphasizes the effectiveness of the ETS end anchorage. The strengthened beams B2F10_A and B2F10_N which have the same area of the BFRP bars showed higher flexural capacities than the strengthened beams B1F14_A and B1F14_N. This may be due to the increase of the surface area of the BFRP bars.

(a) Drilled a hole with 45o angle

(b) Inclined hole (45o)

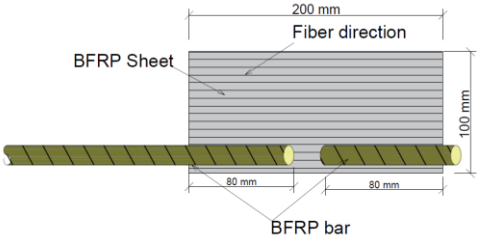


(c) dimension of ETS anchor

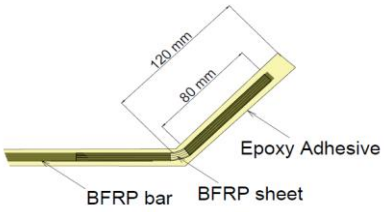


(d) proposed shape of ETS anchor

(e) Impregnated BFRP sheet and BFRP bars before wrapping

(f) Final shape of ETS anchor

**Fig. 3: Manufacturing the ETS end anchorage**

**Fig. 4: Installation of the anchored BFRP bar**

**Table 5: Test results**

| Designation of specimen | Ultimate Load (Pu) kN | Deflection at Pu (mm) | % Increase in ultimate load | Failure mode a |
|---|---|---|---|---|
| BC | ١٣٥,١٣ | 56.50 | --- | DF |
| B1F14_N | 158.75 | 32.22 | 17.48 | BEID |
| B2F10_N | 177.55 | 43.78 | 31.39 | BECCS |
| B1F14_A | 167.5 | 23.68 | 23.95 | IDSB-A |
| B2F10_A | 192.5 | 30.95 | 42.46 | IDSB&R |

[a] DF, BEID, BECCS, IDSB-A, and IDSB&R correspond to ductile failure, bar end interfacial debonding, bar end concrete cover separation, interfacial debonding between BFRP sheet and BFRP bar at anchorage, interfacial debonding between sheet and bars followed by BFRP sheet rupture

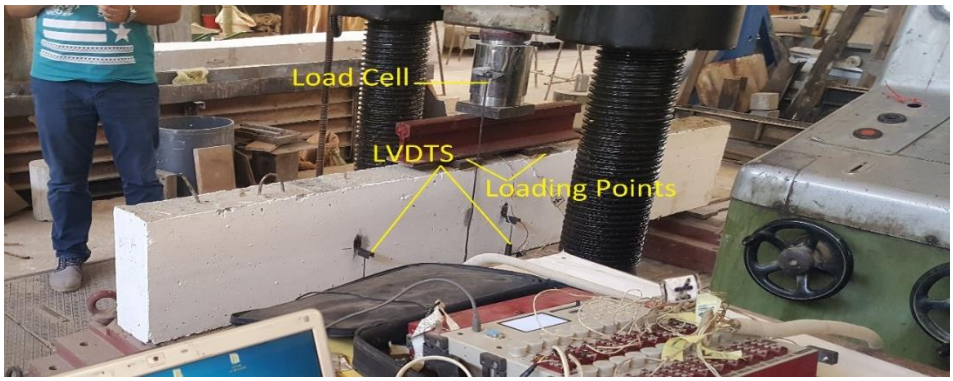


**Fig. 5: Set-up for four-point bending test in laboratory**

### Load-Deflection Curve

The load-midspan deflection behavior of the different beams is presented in Fig. 6. Prior to the yield loads, the behaviors of different beams are almost similar to that of the unstrengthened beam "BC". This behavior suggested that BFRP bars contribute a little to flexural stiffness of strengthened beams before the yield points as shown in Fig. 6. This may be due to a small difference in axial stiffness of BFRP bars before yielding, as seen in Table 4. However, after yield points, post-yield flexural stiffness and strength of the NSM BFRP-strengthened beams were improved compared to the control beam. Using NSM-BFRP bars with and without end anchorage increased the post-yield flexural stiffness and the ultimate loads of the NSM-strengthened beams. Interestingly, the improvement in post-yield flexural stiffness depends on the presence of the ETS end anchorage. Beams B1F14_A and B2F10_A have a steeper slope compared to their counterpart beams without end anchorage, as shown in Fig. 6. The post-yield flexural stiffness of BFRP-strengthened beams with end anchorage increased by 95% compared with counterparts without end anchorage. Moreover, the gained strength of BFRP-strengthened beams is dependent on the surface area of the NSM bars and the number of anchors as shown in Fig. 6, where beams B2F10_N and B2F10_A have higher strength compared to their counterpart beams, B1F14_N and B1F14_A. The minor variations between post-yield flexural stiffnesses of beams strengthened with two BFRP-10 bars and those strengthened with one BFRP-14 bar arise from a small difference in axial stiffness of BFRP bars, as seen in Table 4 .

### Failure Modes of The Tested Beams

The failure modes and the crack pattern of NSM-BFRP strengthened beams differed from those of the unstrengthened beam, as shown in Fig. 7. The failure modes of different beams are listed in Table 5. Crack pattern of the strengthened beams has a smaller cracking amplitude, smaller crack numbers, and wider crack bandwidth compared with that of the control beam. The use of

NSM BFRP bars had resulted in delaying the growth of crack formation and the composite action between BFRP bars and concrete changed the failure mode from flexural failure (Ductile Failure, DF) in case of control beam (BC) to a sudden failure for the strengthened beams. The cracks of strengthened beams propagated and changed to shear cracks until reaching the end of the BFRP bars. These cracks widened until the end zone of the BFRP bars failed, followed by concrete cover separation for the different strengthened beams. This type of debonding was caused by large shear stresses at the end of the BFRP bar/s.

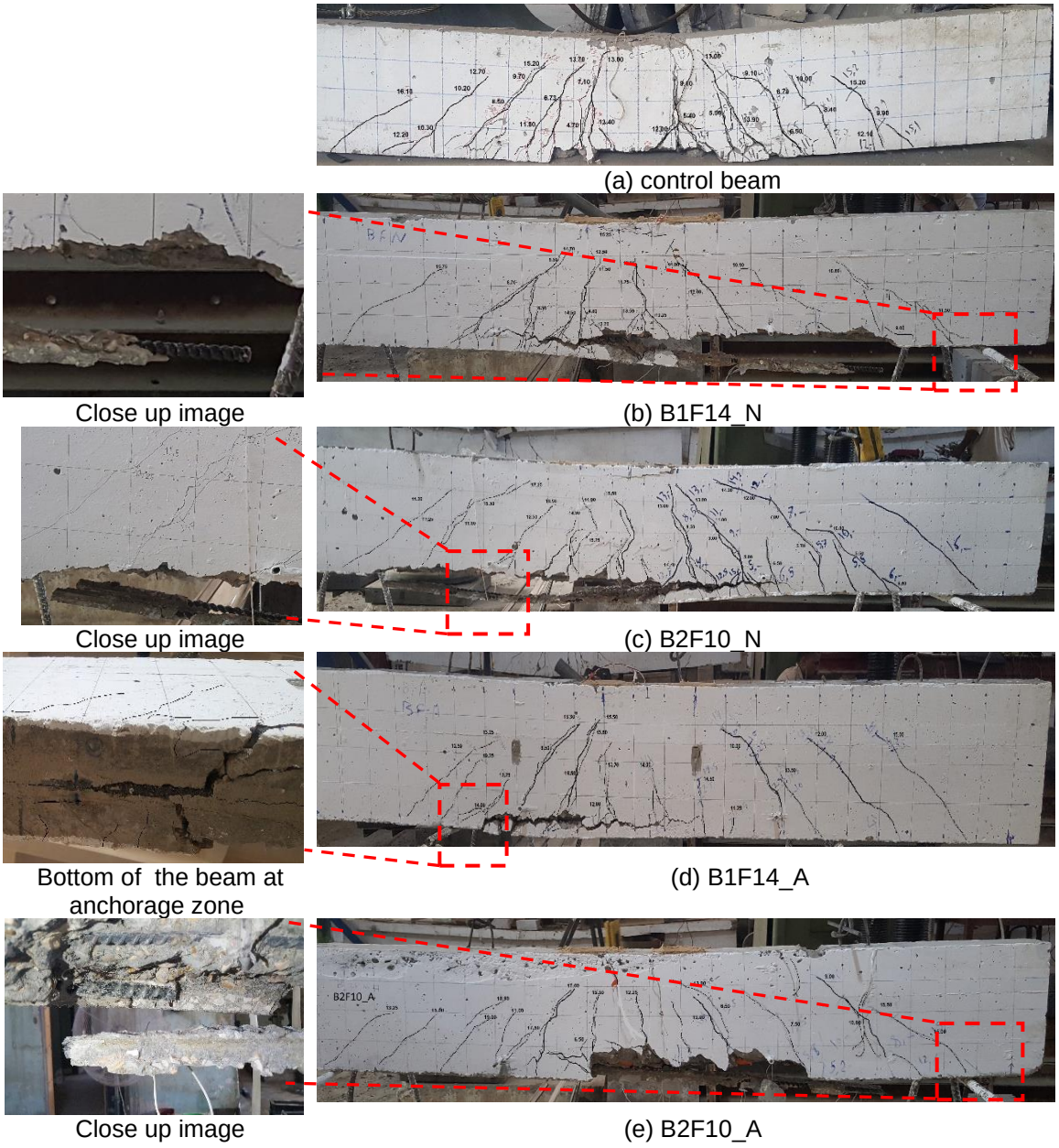


**Fig. 7: Failure modes of the tested beams**

It was obvious that debonding of beam B1F14_N was initiated at the end of the BFRP bar due to Bar End Interfacial Debonding (BEID) between bar and adhesive at a load of 158.75 kN, as shown in Fig. 7b. Beam B2F10_N strengthened by two BFRP-10 bars without anchorage failed also due to Bar End Concrete Cover Separation (BECCS) at the end of the BFRP bars at a load of 177.55 kN. Increasing the number of NSM BFRP bars with the same axial stiffness increased the surface area of the BFRP bars, in turn increasing the bond capacity at the ends which

change the failure mode from interfacial end debonding to concrete cover separation, as shown in Fig. 7c .

The ETS end anchorage technique increased the ultimate loads of the strengthened beams. Nevertheless, use of this anchorage could not fully develop the BFRP tensile strength and the failure of the beams started from the failure of the anchorage system, as shown in Fig. 7(d and e). Beam B1F14_A failed because of slippage between BFRP sheet and BFRP bar at a load of 167.5 kN (Fig. 7d). Thus, complete interfacial debonding between BFRP sheet and BFRP bar "IDSB-A" occurred at the anchorage end. Beam B2F10_A strengthened by two BFRP-10 bars with ETS end anchorage failed due to interfacial debonding between sheet and bars and tearing of the BFRP sheet at the anchorage, followed by rupture "IDSB&R" of anchorage sheets at corners at a load of 192.5 kN, as shown in Fig. 7d. Rupture of fibers at anchorage resulted from stress concentration at corners. This type of failure can be delayed by increasing the curvature at the corners of the anchor. The failure mechanism of the anchorage for both beams commenced as a result of the unconfinement effect between BFRP sheet and bars as the sheet fiber was in the longitudinal direction of the bars. This type of failure could be prevented if another layer of the sheet was wrapped circularly around the bar or by using a bidirectional fiber sheet to increase the circumferential effect. The failure mode of the anchorage fibers' fracture at the corner had a higher load capacity .

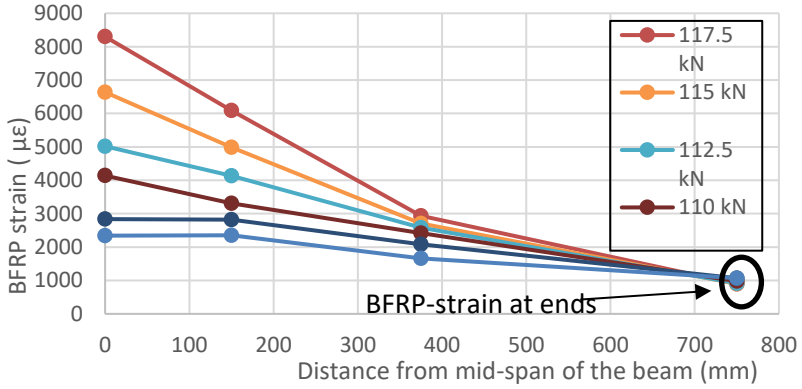


(a) Beam B1F14_N

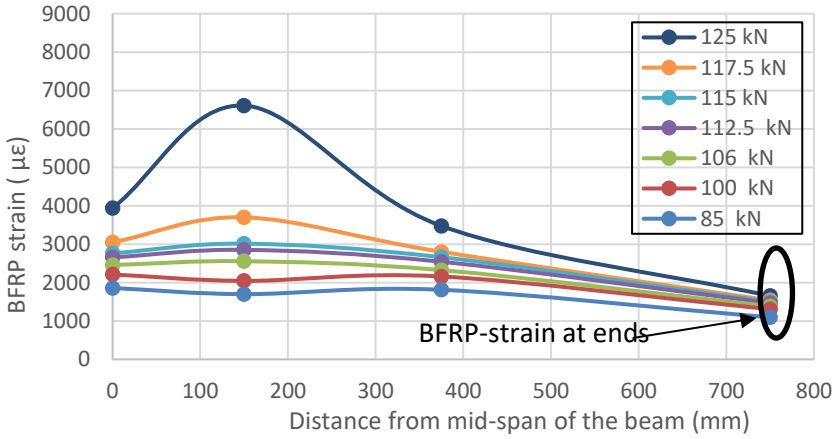


(b) Beam B1F14_A

**Fig. 8: Strain distribution along the bonded length of the BFRP bar**

**BFRP Strain Distribution Along The NSM Bars**

The strain distribution along the length of the BFRP bars at different stages of loading of beams B1F14_N and B1F14_A are presented in Fig.8. The distance is measured from the midspan of the beam, meaning that the middle of the beam corresponds to a zero-millimeter distance along

the BFRP bar. The vertical axis represents the values of BFRP strains obtained from strain gauges attached to bars at different distances as shown previously. Some of the strain gauges attached to the BFRP bars were destroyed during the test and could not capture strain until failure, similar to that behavior observed by Diab and Sayed [23] because of the ripped BFRP bars. Therefore, the strain distribution of the load levels could not be represented until the failure of the beams .

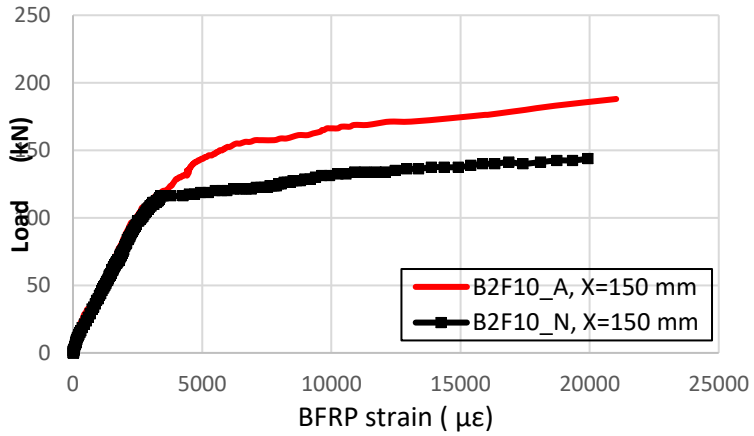


(a) BFRP strain gauges at distance 150 mm

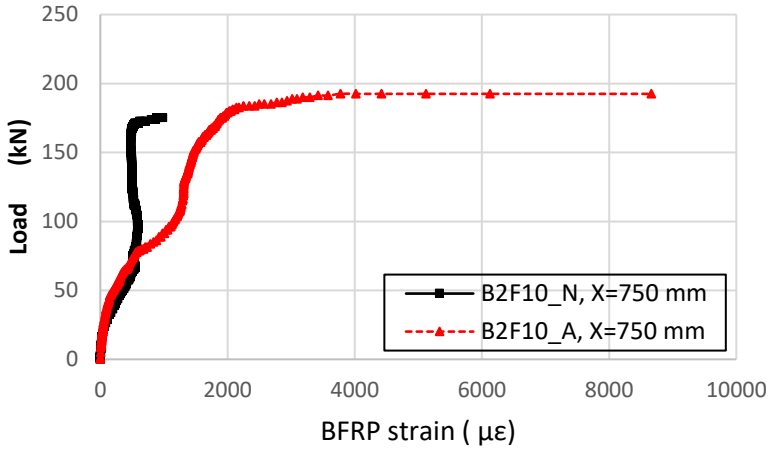


(b) BFRP strain gauges at distance 750 mm

**Fig. 9: A comparison between load and BFRP strain relationship of the beams B2F10_N and B2F10_A at different location**

Prior to cracking loads, the strain distribution along the length of the BFRP bar is observed to follow a nonlinear descending trend and the peak strains were recorded at midspan of the beams. However, upon the crack initiation, this trend was changed, and the peak value of strains occurred behind the flexural crack locations. In general, it is interesting to note that the strain distribution trend is dependent on the presence of ETS end anchorage. Beam B1F14_N (Fig. 8a) strengthened by one BFRP-14 bar without end anchorage has higher strain values and a higher disappearance rate compared with beam B1F14_A using ETS end anchorage (Fig. 8b). On the other hand, strain distributions of beam B1F14_A are flattened and the value of strain at the end of the bar increased with increasing the loads level, as shown in Fig. 8b, which contradicted with the behavior of beam B1F14-N without end anchorage .

The relationships representing applied load versus longitudinal strain at different locations along BFRP bars for beams B2F10-N and B2F10-A are presented in Fig. 9(a and b). For both beams,

B2F10-N and B2F10-A, the BFRP strains at x=150 mm are almost the same before steel yielding points, as shown in Fig. 9a. Beyond the yield point, the strains in beam B2F10-N increase more rapidly than those of beam B2F10-A. The BFRP strain at x=150 mm reached to 21000 με at 0.96 of the ultimate load, which represents 91% of the ultimate capacity of the BFRP-10 bar. Based on the strain in BFRP bars, it can be concluded that the ETS end anchorage of the BFRP bar enhances the strength of the beam compared with its counterpart without end anchorage. The performance of BFRP strains at the end of BFRP bars depends on the presence of ETS end anchorage, as shown in Fig. 9b. The presence of ETS end anchorage results in the increase of strain at the end of BFRP bar for beam B2F10-A with increasing the applied load. On the other hand, the strain at the end of BFRP bar for beam B2F10-N increases until a specified load (about 80 kN); afterwards, a relaxation occurs due to the slippage at the end of the BFRP bars. Consequently, a sudden increase in strain was observed before the final failure without gaining reasonable loads. The behavior of strains at the end of BFRP bars of the other beams, B1F14_N and B1F14_A, is similar to that behavior as mentioned previously (Fig. 8(a and b)). The proposed ETS end anchorage resulted in high strains achieved at the ends of BFRP bars of the strengthened beams. The maximum strain at the ETS end anchor reached 8700 με, representing about 40% of the ultimate capacity of the BFRP-10 bar, but the strain at the end of the BFRP without anchorage was at 4% of its ultimate capacity. It is noted that the strain gauge is attached to the BFRP sheet at anchor, that is, just before the bent bar. Generally, beams strengthened with NSM-BFRP bars using ETS end anchorage exhibited higher load and BFRP end strains than their counterparts without anchorage did. Hence, ETS end anchorage enables strengthened beams to bear a higher load .

## CONCLUSIONS

The experimental program was conducted to introduce nonmechanical anchor, ETS end anchorage technique, for beams strengthened in flexure using NSM BFRP bars. Based on the experimental results and observations, the following conclusions can be stated:

- The result of the experimental study indicated that strengthening of RC beams with NSM BFRP bars without end anchorage enhanced the ultimate capacity and the post-yield stiffness compared to the unstrengthened beam.
- The ETS end anchorage increased both ultimate load and post-yield stiffness of strengthened beams compared to their counterparts strengthened without end anchorage.
- The load carrying capacity of NSM BFRP-strengthened beams was increased by up to 31% for beams strengthened without end anchorage and by 43% for beams strengthened with end anchorage .
- Increasing the surface area of BFRP bars with constant axial stiffness enhanced the ultimate load and ductility of strengthened beams with or without end anchorage.
- The ETS end anchorage achieved about 90% of the BFRP tensile strength and the failure occurred due to tearing failure between BFRP sheet and BFRP bars at the end anchorages. Therefore, more studies are needed to optimize the proposed anchorage.

## REFERENCES

1. Coelho M, Sena-Cruz J, Neves L (2015) A review on the bond behavior of FRP NSM systems in concrete. Constr Build Mater 93:1157–69.
2. Lee D, Cheng L, Yan-Gee Hui J (2013) Bond characteristics of various NSM FRP reinforcements in concrete. J Compos Constr 17:117-129.

3. Almusallam TH, Elsanadedy HM, Al-Salloum YA, Alsayed SH (2013) Experimental and numerical investigation for the flexural strengthening of RC beams using near surface mounted steel or GFRP bars. Constr Build Mater 40:145–61.
4. Wu, G, Dong ZQ, Wu ZS., Zhang LW(2013) Performance and parametric analysis of flexural strengthening for RC beams with NSM-CFRP bars. J Compos Constr 18, 04013051.
5. Mukhopadhyaya P, Swamy RN (2001) Interface shear stress: a new design criterion for plate debonding. J Compos Constr 5:35–43.
6. Barros JAO, Ferreira DRM, Fortes AS, Dias SJE (2006) Assessing the effectiveness of embedding CFRP laminates in the near surface for structural strengthening. Constr Build Mater 20:478–91.
7. Sharaky IA, Torres L, Baena M, Miàs C (2013) An experimental study of different factors affecting the bond of NSM FRP bars in concrete, Compos Struct 9:350–365.
8. Sharaky IA, Torres L, Baena M, Vilanova I (2013) Effect of different material and construction details on the bond behaviour of NSM FRP bars in concrete. Constr Build Mater 38:890–902.
9. Shen D, Zeng X, Zhang J, Zhou B, Wang W (2019) Behavior of RC box beam strengthened with basalt FRP using end anchorage with grooving. J Compos Mater 53(23):3307-3324.
10. Kalfat R, Al-Mahaidi R, Smith ST (2013) Anchorage devices used to improve the performance of reinforced concrete beams retrofitted with FRP composites. A state-of-the-art-review. J Compos Constr 17:14-33.
11. Diab HM, Wu ZS, Iwashita K (2009) Short and long-term bond performance of prestressed FRP sheet anchorages. J Eng Struct 31(5):1241-1249
12. Diab HM, Farghal OA (2014) Bond strength and effective bond length of FRP sheets/plates bonded to concrete considering the type of adhesive layer. Compos Part B: Eng 58:618-624
13. Wang Q, Zhu H, Zhang B, Su W (2020) Anchorage systems for reinforced concrete structures strengthened with fiber-reinforced polymer composites: State-of-the-art review. J Reinf Plast Compos 0(0):1–18
14. Li T, Zhu H, Wang Q, Li J (2018) Experimental study on the enhancement of additional ribs to the bond performance of FRP bars in concrete. Constr Build Mater 185:545–554.
15. Reda RM, Sharaky IA, Ghanem M, Seleem MH, Sallam HE (2016) Flexural behavior of RC beams strengthened by NSM GFRP bars having different end conditions. Compos Struct 147:131–142.
16. Sun W, He T, Liu S (2019) Developing an anchored CFRP reinforcement for efficiently and readily strengthening reinforced concrete structures. Compos Part B: Eng 176:107199
17. Sharaky IA, Torres L, Sallam HEM (2015) Experimental and analytical investigation into the flexural performance of RC beams with partially and fully bonded NSM FRP bars/strips. Compos Struct 122:113–126.

18. Wang Q, Zhu H, Li T, Wu G, Hu X (2019) Bond performance of NSM FRP bars in concrete with an innovative additional ribs anchorage system: An experimental study. Constr Build Mater 207: 572-584.
19. Wu G, Dong ZQ, Wu ZS, Zhang L (2013) Performance and parametric analysis of flexural strengthening for RC beams with NSM-CFRP bars. J Compos Constr 18(4): 04013051-10 .
20. Peng H, Zhang J, Cai CS, Liu Y (2014) An experimental study on reinforced concrete beams strengthened with prestressed near surface mounted CFRP strips. Eng Struct 79:222–233.
21. Basim S, Hejazi F, Rashid RSBM (2019) Embedded carbon fiber-reinforced polymer rod in reinforced concrete frame and ultra-high-performance concrete frame joints. Int J Adv Struct Eng 11: 35–51.
22. Breveglieri M, Aprile A, Barros JAO (2015) Embedded Through-Section shear strengthening technique using steel and CFRP bars in RC beams of different percentage of existing stirrups. Compos Struct 126:101-113 .
23. Diab HM, Sayed AM (2020) An anchorage technique for shear strengthening of RC T-beams using NSM-BFRP bars and BFRP sheet. Int. J Concr Struct Mater 14(49):1-16
24. Miskolczi N (2013) Polyester resins as a matrix material in advanced fibre-reinforced polymer (FRP) composites. In: Bai JBT-AF-RP (FRP) C for SA, editor. Woodhead publ. Ser. Civ. Struct. Eng. Woodhead Publishing: 44–68. https://doi.org/10.1533/9780857098641.1.44.
25. Kaya E, Kütan C, Sheikh S, _Ilki A (2017) Flexural retrofit of support regions of reinforced concrete beams with anchored FRP ropes using NSM and ETS methods under reversed cyclic loading. J Compos Constr 21:615–25. https://doi.org/10.1061/(ASCE)CC.1943-5614
26. ASTM A370-97a Standard Test Methods and Definitions for Mechanical Testing of Steel Products, American Society for Testing and Materials (ASTM), West Conshohocken, PA, 1997.
27. Egyptian Code of Practice, ECP 203-2007. Design and Construction for Reinforced Concrete Structures. Ministry of Building Construction, Research Center for Housing, Building and Physical Planning, Cairo, Egypt 2007.
28. Zhejiang Hengdian Imp.&Exp.Co.,Ltd www.basaltfiber-gbf.com(accessed April 14, 2020)
29. Shanxi Basalt Fiber Technology Co., Ltd http://www.sxcbf.com/en/sjxmmore.asp?c_id=48&hiden=39 (accessed April 14, 2020)
30. Sikadur®-30. Product Data sheet-adhesive for bonding reinforcement. Available online: https://egy.sika.com/dms/getdocument.get/a470020f-8c78-314e-89f1-3862b8560f7f/Sikadur%20-30.pdf
31. Sikadur®-330. Product Data sheet-adhesive for bonding reinforcement. Available online: https://egy.sika.com/dms/getdocument.get/b5ed2585-b802-3ef0-8825-c669aa8542e3/Sikadur_330.pdf